The International Journal of Advanced Manufacturing Technology (2022) 120:7937–7949
https://doi.org/10.1007/s00170-022-09302-0

ORIGINAL ARTICLE

Optimization of gas carburizing treatment parameters of low carbon steel using Taguchi and grey relational analysis (TA-GRA)

Sofiane Touati[1] · Laala Ghelani[1] · Amina Zemmouri[2] · Haithem Boumediri[3]

Received: 15 February 2022 / Accepted: 28 April 2022 / Published online: 6 May 2022

Abstract
This work aims to optimize the micro-hardness (H), thickness of the hardened layer (THL), carbon contents (%C) and surface roughness (Ra) of XC10 steel using a gas carburizing thermochemical treatment. The combination of Taguchi and grey relational analysis (TA-GRA) was applied with 9 experiments on the basis of L9 orthogonal design using the following factors: carbon flow rate (0.9%, 1% and 1.2%), temperature (900°, 920° and 940°) and holding time (4 h, 5 h and 6 h). A statistical analysis of the results was carried out on the basis of the *S/N* ratio and an ANOVA to identify the most significant parameters affecting the experimental responses. A desirability function approach was established to find the optimal factors to maximize H, THL and %C and minimize Ra. The gas carburizing treatment has shown a strong increase in the micro-hardness with about 140%, the thickness of the hardened layer with more than 1400 µm, carbon content 775% and good decrease in the surface roughness (Ra) with 140%.

Keywords Gas carburizing of steel · Surface roughness · Thickness of the hardened layer · Micro-hardness · TA-GRA · Desirability function

1 Introduction

Low carbon steels have been commonly used because they guarantee high performances such as good plasticity, toughness and wear resistance. Moreover, it is one of the most used in the national economy, and it is often used after heat or thermochemical treatment [1–3]. Some carbon steel parts (shafts, gears, connecting rods and machine tool parts, etc.) must have enough toughness to resist fatigue (resistance to dynamic loads), tribological properties (resistance to friction and wear) and corrosion (resistance to chemical attack) [4–7]. The surface hardening was an accepted technology around the world because of its cost and its characteristics [8].

Up to date, different methods of cementing with different principles have been studied to produce activated carbon, such as gas carburizing [9], plasma carburizing [10, 11], vacuum carburizing [1], plasma electrolytic carburizing [12], electron beam carburizing [13] and laser carburizing [14].

In gas carburizing, the surface of low carbon steel can be enriched with carbon up to 1% (weight) [15, 16]. The increase of the surface layer with the carbon content shows the transformation of austenite into martensite and finally formation of cementite (Fe_3C) [17–19]. Furthermore, there are a lot of transformations in the core of the samples; ferrite and pearlite (initial phase) are transformed into retained austenite and bainite (after treatment phase) [20–22]. After thermochemical case hardening, if the steels are cooled in the furnace, an accumulation of thick and hard layers of cementite will occur within the grain boundaries, so case hardening without quenching and tempering has several drawbacks [21, 23, 24].

The case hardening treatment was carried out between 880 and 950 °C to improve the surface hardness of the steel parts, resulting in case hardened layers of up to 20–25% [25, 26]. The researchers have shown that the outer layer of the steel is characterized by a higher hardness when there is a similar increase in

✉ Haithem Boumediri
haithem.boumediri@yahoo.com

1 Mechanical Engineering Department, University Abbes Laghrour, BP. 1252, 40004 Khenchela, Algeria

2 Mechanical Engineering Department, Mechanics of Materials and Plant Maintenance Research Laboratory (LR3MI), Badji Mokhtar University, BP.12, 23052 Annaba, Algeria

3 Laboratoire de Mécanique Appliquée Des Nouveaux Matériaux (LMANM), Université 8 Mai 1945, BP. 401, 24000 Guelma, Algeria

Table 1 The chemical composition of steel XC10 (weight %)

Element	C	Mn	Si	S	Cu	AL	Ti	Ni	Cr	Mo	Sn	W	Co	Ta	N	Fe
Weight %	0.10	0.50	0.31	0.010	0.047	0.003	0.003	0.033	0.087	0.012	0.015	0.018	0.09	0.073	0.051	98.7

carburation time [17, 26, 27]. In order to obtain a hard, wear and fatigue-resistant outer surface, it is necessary to choose the right type of steel to match with the appropriate treatment method [28]. The surface roughness parameters are very important factors to affect the micro-pitting life [29, 30]. Sougata and Zhe have shown that the case carburizing treatment and especially the holding time influence the surface roughness [31, 32].

Taguchi's method is one of the optimization and statistical tools used to classify the factors that influence the experimental responses (most significant, least significant and non-significant) [33–35]. As the use of this method is mainly applicable for experimental treatments [36–38], it can also be used for numerical and theoretical analyses [39, 40]. However, to optimize the parameters that influence the responses, a further study involving the use of Taguchi analysis as well as grey relational analysis (GRA) to obtain the order (rank) of the importance of each process factor is needed [41, 42].

This study aims to optimize the parameters of the thermochemical gas carburizing treatment such as carbon flow rate, temperature and holding time, to see their influences on the surface micro-hardness of the steel (HV), thickness of the hardened layer (THL), carbon contents (%C) and surface roughness (Ra) using the Taguchi-based GRA method. In addition, the analysis of variance (ANOVA) was used to determine the influence of each parameter on the responses. To the author's knowledge, a very few studies have adopted the TA-GRA (Taguchi + GRA) analysis in the field of thermochemical treatment and specifically gas carburizing to better measure the quality of the phenomenon. Finally, the microstructure of XC10 steel was investigated by spark optical emission spectroscopy to see the transformation of austenite to martensite and then into cementite (Fe_3C).

2 Materials and methods

2.1 Materials

The material used in this study is a low carbon steel (XC10) whose chemical composition is shown in Table 1. Figure 1 shows the manufacture of the primary samples which were obtained by lubricated cutting of a cylindrical bar with a diameter of 55 mm and a thickness of 10 mm, using an SN-40 lathe.

2.1.1 Thermochemical treatment (gas carburizing)

The heat treatment of the samples was carried out on a line consisting of a carburizing furnace, a hardening oven, an oil-quenching bath and a washing system. The line is controlled by the Axron Swiss Process Control software. First, the samples were prepared on a hanging stainless-steel pot rack. Then, the samples were introduced into the bell furnace (type 11-CG, SOLO-Swiss, Switzerland) with an atmosphere consisting of a carrier gas made up of 39.36% of H_2, 0.23% of CO_2, 19.83% of CO and 0.76% of $\%H_2O$, enriched in propane C3H8. The samples were processed by the gas carburizing treatment according to the following factors: carbon flow rate (A), temperature (B) and holding time (C) where each factor has three levels as summarized in Table 2.

Fig. 1 Preparation of samples

After the sample surfaces are enriched with carbon, a diffusion step is required for 90 min to ensure that the carbon is diffused evenly over the surface of the workpiece, followed by a quenching treatment at 830 °C for 20 min. Thereafter, the specimens throw a tank of oil at 60 °C for 18 min; afterward, they dried in a drying machine for 25 min. Finally, the samples were annealed at a temperature of 180 °C for 120 min.

The carbon penetration into the steel depends on time and temperature selected during carburizing. Fick's second law generally satisfies the relationship between the thickness of the carburized layer and carburizing time; it is defined as follows [43]:

$$\frac{\delta C_x}{\delta t} = D\frac{\delta^2 C_x}{\delta x^2} \tag{1}$$

where C_x is the concentration at distance x from the surface, t is the time, D is the diffusion coefficient, $\frac{\delta C_x}{\delta t}$ is the variation of the volume concentration as a relation to time t, and $\frac{\delta^2 C_x}{\delta x^2}$ is the concentration gradient varies with distance x.

As the hardness of steel increases, the carbon atoms vary with their absorption from the atmosphere by the hardness surface layer, which is estimated by the micro-hardness distributions. In some cases, the case carburizing process can be defined by the Van Ostrand-Dewey diffusion formula [44]:

$$\frac{C_s - C_x}{C_s - C_o} = erf\left(\frac{x}{2(Dt)^{1/2}}\right) \tag{2}$$

where C_s is the superficial carbon concentration and C_o is the initial concentration of the carbon in the base steel.

2.1.2 Microscope

The micrographs were captured using digital camera AxioCam MRc 5 attached to a Leica DMi8 inverted microscope (Leica Microsystems CMS GmbH, Wetzlar, Germany), and the thickness layer of the samples was performed in three different points by Leica IM50 software3.

2.1.3 Micro-hardness measurements

The Vickers micro-hardness tester measurements were performed under a test load of 0.5 kgf and a 10-s dwell time, using a micro-hardness tester by Zwick Roell, model: ZHV10-A. The test was performed at a room temperature and hardness measurements were taken to five different locations on each sample to obtain an average hardness value.

Table 2 Formulation of test input parameters and their level

Parameter	Symbol	Level		
		Min (−1)	Medium (0)	Max (+1)
Carbon flow rate (%)	A	0.9	1	1.2
Temperature (°C)	B	900	920	940
Holding time (h)	C	4	5	6

2.1.4 Spark optical emission spectroscopy

The chemical composition of the steel XC10 samples before and after the case hardening treatment was conducted by spark optical emission spectroscopy (S-OES) using a SPECTROMAXx MX6M-BT metal analyzer from SPECTRO Analytical Instruments GmbH, and it is given in mass percent throughout this work. The tests were measured under an argon atmosphere at a pressure of 3 bar during the chemical analysis. The values indicated correspond to the average of at least three individual measurements.

2.2 Methods

2.2.1 Taguchi method

In this study, a Taguchi design plan was used to minimize the number of experiments from 27 to 9 experiments, where each experiment contains five samples. The signal-to-noise ratio (*S*/*N*) can be used to analyze experimental results, that assess the influence of factors and their levels on the response by measuring the difference between the answer and the expected value [45, 46]. There are three types of *S*/*N* ratios to find the best experimental results. The larger is better (LB), the nominal is best (NB) and the smaller is better (SB).

In the current study, the larger is better was used for hardness, thickness of the hardened layer and carbon contents, but the smaller is better was used for the surface roughness. The corresponding *S*/*N* ratio can be expressed and calculated as a logarithmic transformation using the following equation [47]:

$$S/N_{\text{Larger}} = -10\log_{10}\left[\frac{1}{n}\sum_{i=1}^{n}\frac{1}{Y_i^2}\right] \tag{3}$$

$$S/N_{\text{Smaller}} = -10\log_{10}\left[\frac{1}{n}\sum_{i=1}^{n}Y_i^2\right] \tag{4}$$

where the *S*/*N* is the signal-to-noise ratio (dB), n is the number of repetitions for each experiment and Y is the response values obtained during the tests.

ANOVA analyses were performed to determine the most influential factors in the responses [48]. The F-value and P-value were used in the ANOVA to test the significance of each parameter in all responses in this study. Then, linear regression analysis was used to create mathematical regression models for each response against the independent factors. Furthermore, the optimum parameter levels were determined by the desirability function to obtain simultaneous maximization

of micro-hardness, thickness of the hardened layer and carbon contents and minimization of surface roughness (Ra).

2.2.2 Grey relational analysis method

A grey relational analysis (GRA) starts by standardizing the results within a range of 0 to 1, commonly known as the grey relational generation. Then, the grey relational factor between all the reference sequences and the base sequence is established to define the correlation between the data of the desired (ideal/best) and the actual experimental values. Finally, the grey relational score is established by averaging the grey relational score of each response.

The overall ranking of the different responses is determined by the grey relational score. The grey relational score thus makes it possible to optimize many responses by transforming them into a single grey relational score. The estimated grey relational score ranges from 0 to 1, and the larger the value, the closer it is to the idle value. Of all the combinations of process variables used, the one with the highest degree of grey relational score between the reference sequence and itself is judged to be the correct parametric combination and therefore recommended. If a higher value indicates a better performance such as hardness, thickness of the hardened layer and carbon contents, it is normalized according to the following equation [49]:

$$X_{ij} = \frac{Y_{ij} - \mathrm{Min}\left[Y_{ij}, i = 1,2,3 \ldots n\right]}{\mathrm{Max}\left[Y_{ij}, i = 1,2,3 \ldots n\right] - \mathrm{Min}\left[Y_{ij}, i = 1,2,3 \ldots n\right]} \tag{5}$$

If a lesser value indicates a better performance such as surface roughness (Ra), it is explained as follows:

$$X_{ij} = \frac{\mathrm{Max}\left[Y_{ij}, i = 1,2,3 \ldots n\right] - Y_{ij}}{\mathrm{Max}\left[Y_{ij}, i = 1,2,3 \ldots n\right] - \mathrm{Min}\left[Y_{ij}, i = 1,2,3 \ldots n\right]} \tag{6}$$

The relational grey coefficient can be determined as follows:

$$Y\left(X_{oj}, X_{ij}\right) = \frac{\nabla_{\min} + \zeta \nabla_{\max}}{\nabla_{ij} + \zeta \nabla_{\max}} \left[i = 1,2,3 \ldots ., n \text{ and } j = 1,2,3 \ldots ., m\right] \tag{7}$$

where $\nabla_{ij} = \left[X_{oj} - X_{ij}\right]$, $\nabla_{\min} = \mathrm{Min}\left[\nabla_{ij}, [i = 1,2,3 \ldots ., n \text{ and } j = 1,2,3 \ldots ., m]\right]$ and $\nabla_{\max} = \mathrm{Max}\left[\nabla_{ij}, [i = 1,2,3 \ldots ., n \text{ and } j = 1,2,3 \ldots ., m]\right]$ ζ is the distinguishing coefficient that is defined in the range 0 to 1.

Generally, the distinctive coefficient can be adjusted to fit the practical requirements. Considering micro-hardness, thickness of the hardened layer, carbon contents and surface roughness (Ra), both are given equal weights that assume a value of 0.5. The grey relational grade can be expressed as follows:

Table 3 L9 design of experiments established using Taguchi method and their experimental average values with their signal/noise ratios

Run	Codified values			Carbon flow rate (%)	Temperature (°)	Holding time (h)	Micro-hardness (HV)	*S/N* stress (dB)	Thickness of the hardened layer (µm)	*S/N* stress (dB)	Roughness (Ra) (µm)	*S/N* stress (dB)	Carbon contents (%)	*S/N* stress (dB)
	X_1	X_2	X_3											
Raw	–	–	–	–	–	–	336 ± 5	–	–	–	1.433 ± 0.208	–	0.10 ± 0.005	–
1	−1	−1	−1	0.9	900	4	581 ± 5	34.67	1044.76 ± 6.81	60.38	0.912 ± 0.008	0.80	0.548 ± 0.013	−5.22
2	−1	0	0	0.9	920	5	664 ± 10	35.34	1175.80 ± 2.88	61.41	0.683 ± 0.029	3.31	0.558 ± 0.033	−5.06
3	−1	1	1	0.9	940	6	782 ± 16	36.03	1361.15 ± 19.89	62.68	0.525 ± 0.025	5.60	0.555 ± 0.015	−5.10
4	0	−1	0	1.0	900	5	637 ± 5	35.14	1110.35 ± 7.17	60.91	0.780 ± 0.026	2.16	0.628 ± 0.023	−4.03
5	0	0	1	1.0	920	6	751 ± 8	35.87	1287.96 ± 4.27	62.20	0.577 ± 0.032	4.78	0.698 ± 0.021	−3.11
6	0	1	−1	1.0	940	4	702 ± 14	35.64	1232.61 ± 10.97	61.82	0.705 ± 0.013	3.036	0.613 ± 0.024	−4.24
7	1	−1	1	1.2	900	6	764 ± 15	35.94	1275.40 ± 2.97	62.11	0.607 ± 0.038	4.34	0.891 ± 0.011	−1.00
8	1	0	−1	1.2	920	4	668 ± 16	35.37	1230.37 ± 1.66	61.80	0.730 ± 0.02	2.73	0.812 ± 0.016	−1.80
9	1	1	0	1.2	940	5	815 ± 15	36.19	1419.04 ± 7.13	63.04	0.597 ± 0.032	4.49	0.875 ± 0.030	−1.15

$$\Gamma\left(X_o, X_i\right) = \frac{1}{m}\sum_{i=1}^{m} Y\left(Y_{oj}, Y_{ij}\right) \quad (8)$$

where m is the number of response parameter.

3 Results and discussion

The average experimental values of 5 samples for each combination obtained by the Taguchi method with their signal/noise ratios in relation with the micro-hardness, thickness of the hardened layer, carbon contents and surface roughness (Ra), for the different combinations of the gas carburizing treatment parameters and according to the experimental design L9, are presented and compared with the raw in Table 3. The micro-hardness values obtained in this study show an increase of more than 140% from 336 ± 5 HV to 815 ± 15 HV. These established values are higher than those found by several authors, who have reported an increase in micro-hardness of around 80% [50, 51]. The found values for the thickness of the hardened layer are between 1044.76 ± 6.81 µm and 1419.04 ± 7.13 µm. These values are greater than those reported by several authors, which found that the thickness of the hardened layer resulted is in the range of 1000 µm and 1300 µm [22, 52]. The obtained carbon content values show an increase from 0.1 to 0.875% which means an increase of about 775%. These values are high compared to those found in the literature by several authors, such as Hiremath et al. [53] and Oyetunji and Adeosun [54], where the maximum carbon content found was 0.8%. The surface roughness (Ra) improved from 1.433 to 0.597 µm, which means an improvement of 140%. These values have given some importance to those found by several authors Liu et al. [31] and Roy et al. [32].

Figure 2a shows that the carbon flow has a positive effect on the micro-hardness, thickness of the hardened layer, carbon contents and surface roughness (Ra) with 9.78%, 8.74%, 35.53% and 8.82% respectively. This study was also validated

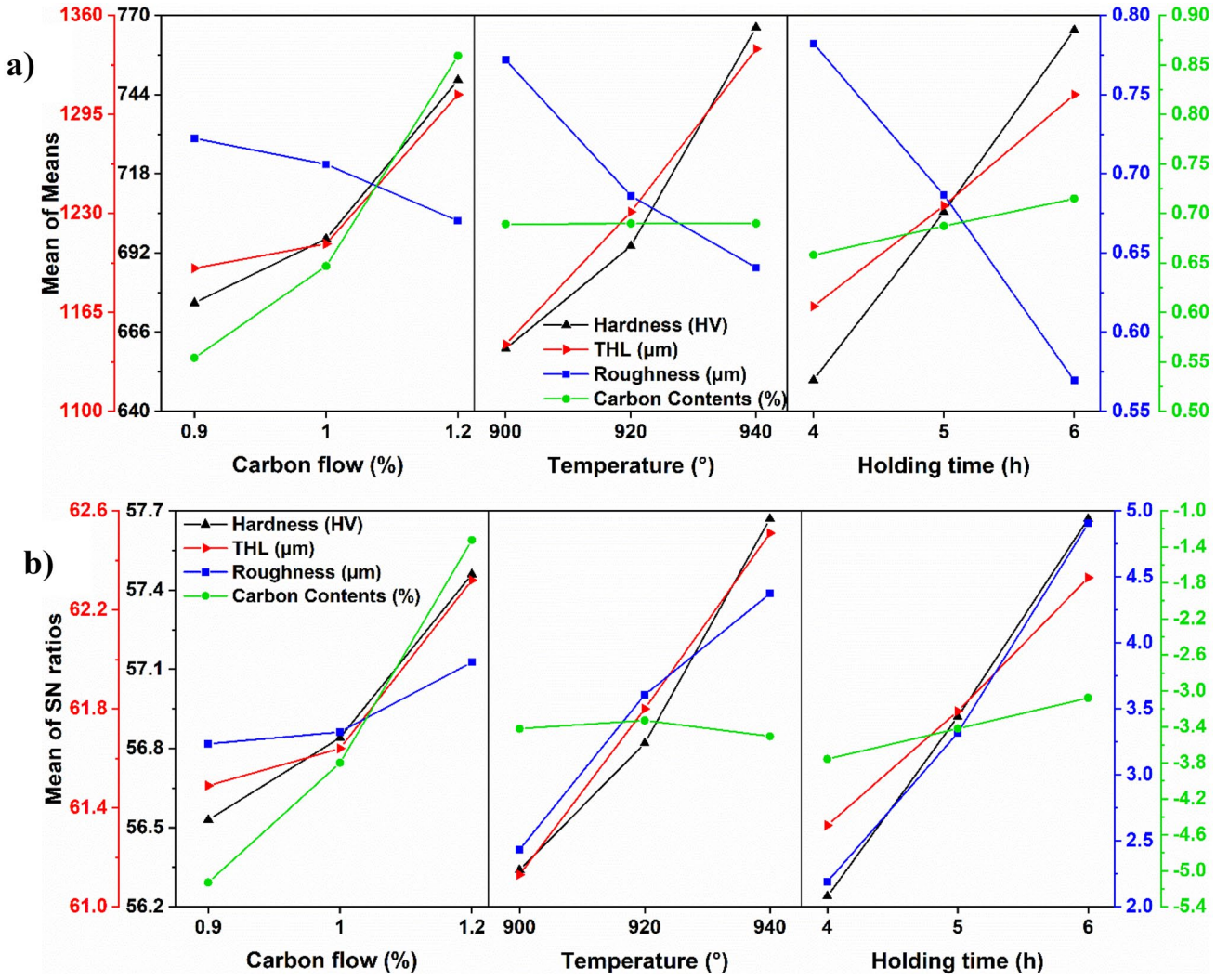

Fig. 2 Taguchi design result for the hardness, Thickness of the hardened layer, carbon contents and surface roughness (Ra). **a** Main effect plot means and **b** main of *S*/*N* ratio

by Dechow and Douglas [55]. Regarding the temperature parameter which has a significant influence on the responses such as micro-hardness, thickness of the hardened layer and surface roughness (Ra) at 13.76%, 14.51% and 20.53% respectively, but it has a weak effect on the carbon contents (%) at 1.15%. This result was also confirmed by Li et al. [25] and Oyetunji [56]. Finally, the holding time has a great influence on the micro-hardness, thickness of the hardened layer and surface roughness (Ra) by 15.01%, 10.62% and 27.21% respectively, except that the influence of this parameter is less significant on the carbon contents with 7.84%. Benarioua [17] and Abdenour et al. [22] showed a significant increase in the micro-hardness, thickness of the hardened layer and carbon contents.

Figure 2b gives the influence of the average signal-to-noise ratio (*S*/*N*) on the micro-hardness, thickness of the hardened layer, carbon contents and surface roughness (Ra). It can be seen that the carbon flow rate, temperature and holding time have a main effect on the previous responses, only for the carbon content, which is less affected by the temperature and holding time.

3.1 Analysis of variance

Table 4 presents the ANOVA analysis of micro-hardness, thickness of the hardened layer, surface roughness (Ra) and carbon percentage. The *P*-value shows that there is a statistical significance in the responses since it is much lower than 0.05 [38, 57]. Only the temperature parameter is not statistically significant in the carbon content because the *P*-value greater than 0.7. The average experimental results in terms of these models are statistically tested to identify the most significant variables that act to improve the measured responses. In other words, the model can be confirmed by the highest correlation coefficients (R^2, adjusted R^2 and predicted R^2), which corresponds to the established selection criteria.

Regarding the effect of the parameters *A*, *B* and *C* on micro-hardness. The holding time (*C*) and temperature (*B*) have the

Table 4 ANOVA for the linear model of hardness, thickness of the hardened layer, surface roughness and carbon contents

Source		DF	Adj SS	Adj MS	F-Value	P-Value	Cont %	Remark
Micro-Hardness	**Model**	3	44984	14994.7	54.25	<0.001	97.01%	Significant
	A: Carbon flow rate	1	8503	8502.9	30.77	0.003	18.33%	Significant
	B: Temperature	1	16679	16678.9	60.35	0.001	35.97%	Significant
	C: Holding time	1	19802	19802.2	71.65	<0.001	42.70%	Significant
	Error	5	1382	276.4				
	Total	8	46366					
	Fit Statistics	**R²** = 0.9702;		**Adjusted R²** = 0.9523;			**Predicted R²** = 0.8778	
Thickness of the hardened layer	**Model**	3	107494	35831.2	92.81	<0.001	98.24%	Significant
	A: Carbon flow rate	1	22035	22035.3	57.08	0.001	20.14%	Significant
	B: Temperature	1	56510	56510.0	146.38	<0.001	51.64%	Significant
	C: Holding time	1	28948	28948.4	74.98	<0.001	26.45%	Significant
	Error	5	1930	386.1				
	Total	8	109424					
	Fit Statistics	**R²** = 0.9824;		**Adjusted R²** = 0.9718;			**Predicted R²** = 0.9296	
Surface Roughness	**Model**	3	0.1112	0.0370	66.80	<0.001	97.56%	Significant
	A: Carbon flow rate	1	0.0061	0.0061	10.98	0.021	5.35%	Significant
	B: Temperature	1	0.0371	0.0371	66.91	<0.001	32.57%	Significant
	C: Holding time	1	0.0680	0.0680	122.51	<0.001	59.66%	Significant
	Error	5	0.0028	0.0005				
	Total	8	0.1140					
	Fit Statistics	**R²** = 0.9757;		**Adjusted R²** = 0.9611;			**Predicted R²** = 0.9146	
Carbon Contents	**Model**	3	0.1518	0.0506	89.19	<0.001	98.16%	Significant
	A: Carbon flow rate	1	0.1469	0.1469	258.89	<0.001	94.97%	Significant
	B: Temperature	1	0.0001	0.0001	0.16	0.702	0.06%	No-significant
	C: Holding time	1	0.0048	0.0048	8.52	0.033	3.13%	Significant
	Error	5	0.0028	0.0006				
	Total	8	0.1546					
	Fit Statistics	**R²** = 0.9817;		**Adjusted R²** = 0.9707;			**Predicted R²** = 0.9357	

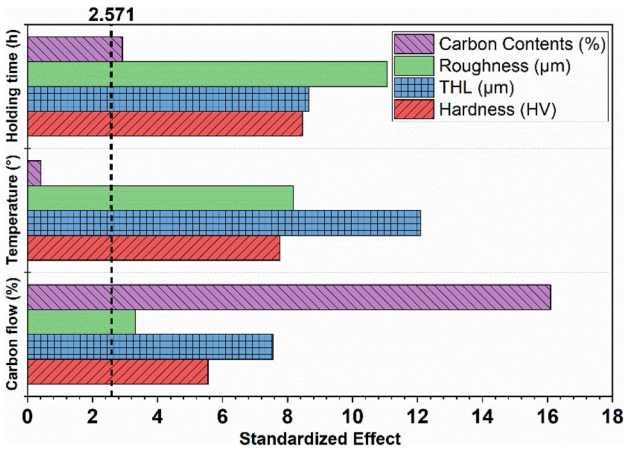

Fig. 3 Pareto diagram of standardized effects on micro-hardness, thickness of the hardened layer, roughness and carbon contents

biggest contribution values of 42.70% and 35.97% respectively, but the carbon flow rate (*A*) has a less contribution with 18.33%. For the thickness of the hardened layer, the temperature (*B*) has the largest contribution value of 51.64%; besides, the effect of holding time (*C*) and carbon flow rate (*A*) contributes with 26.45% and 20.14% respectively. About the surface roughness (Ra), the holding time (*C*) and temperature (*B*) have the greatest contribution with 59.66% and 32.57% respectively. The effect of carbon flow rate (*A*) contributes slightly to the roughness of the surface (Ra) with 5.35%. In addition, the carbon flow rate (*A*) has the most contribution carbon contents with 94.97% and the effect of holding time (*C*) contributes slightly with less than 3.2%. The temperature parameter has a negligible contribution to the carbon contents.

Multiple linear regression models were obtained using Minitab18 software for micro-hardness (Y_1), thickness of the hardened layer (Y_2), surface roughness (Ra) (Y_3) and carbon contents (Y_4). The completes models can be given by the following equations:

$$Y_{1\,\text{Micro Hardness}\,(HV)} = -2260 + 264.4 \times A + 2.636 \times B + 57.45 \times C \quad (9)$$

$$Y_{2\,\text{Thickness}\,(\mu\text{m})} = -3984 + 396.7 \times A + 4.852 \times B + 69.46 \times C \quad (10)$$

$$Y_{3\,\text{Surface Roughness}\,(\mu\text{m})} = 5.046 - 0.2087 \times A - 0.003933 \times B - 0.10644 \times C \quad (11)$$

$$Y_{4\,\text{Carbon Contents}\,(\%)} = -0.332 + 1.0243 \times A - 0.000197 \times B + 0.02839 \times C \quad (12)$$

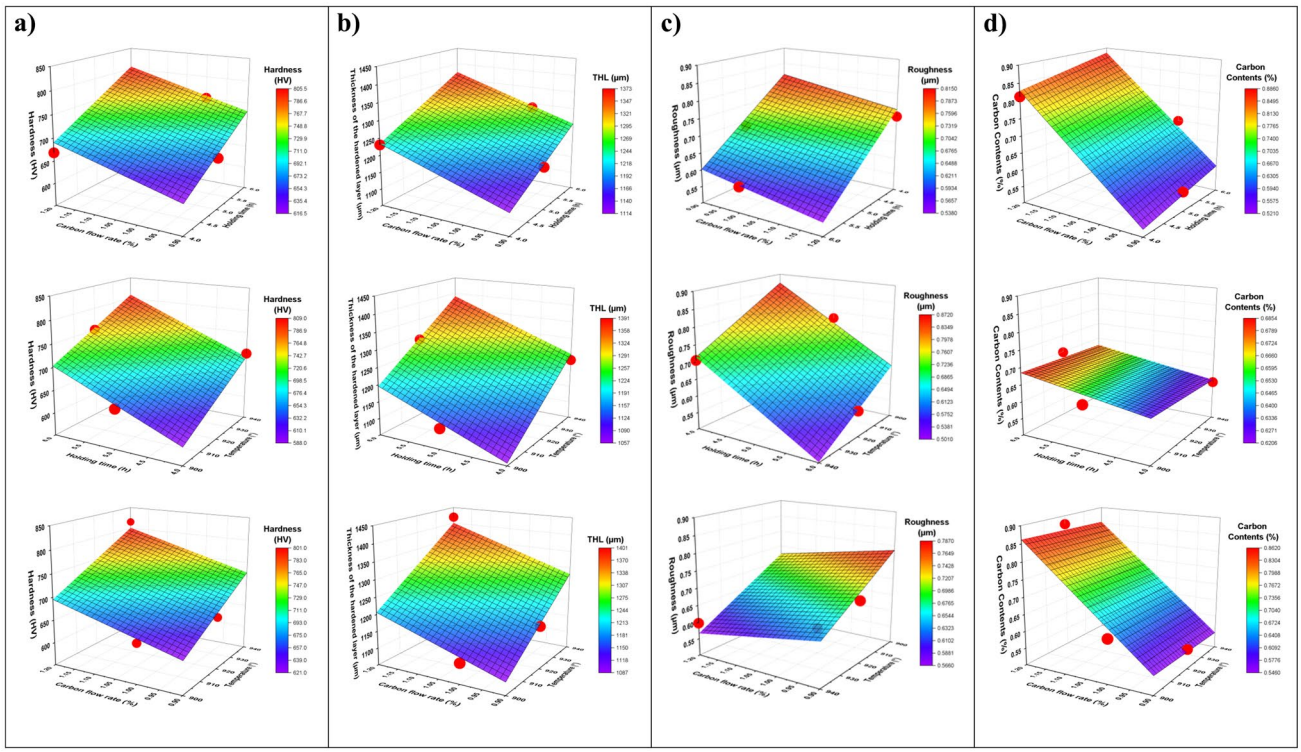

Fig. 4 3D plots showing the effect of the input parameters and their interactions of **a** micro-hardness, **b** thickness of the hardened layer, **c** roughness and **d** carbon contents

Table 5 The best solutions for the gas carburizing treatment parameters with their related responses

Solution	Carbon flow rate (%)	Temperature (°C)	Holding time (h)	Micro-hardness (HV)	THL (µm)	Carbon contents (%)	Roughness (Ra) (µm)	Composite desirability
1	1.20	929.50	6.00	830.57	1419.15	0.883	0.50	0.995
2	1.20	940.00	6.00	858.27	1470.12	0.881	0.46	0.993
3	1.14	940.00	6.00	843.03	1445.59	0.818	0.47	0.942
4	1.20	940.00	4.29	760.13	1351.47	0.833	0.64	0.777
5	1.01	940.00	6.00	810.54	1393.32	0.68	0.50	0.775
6	1.20	940.00	4.01	743.90	1331.84	0.83	0.67	0.720
7	1.20	916.47	4.01	681.75	1217.53	0.83	0.76	0.500
8	1.20	916.33	4.01	681.39	1216.86	0.83	0.76	0.499
9	1.20	900.00	4.01	638.61	1137.94	0.83	0.83	0.324

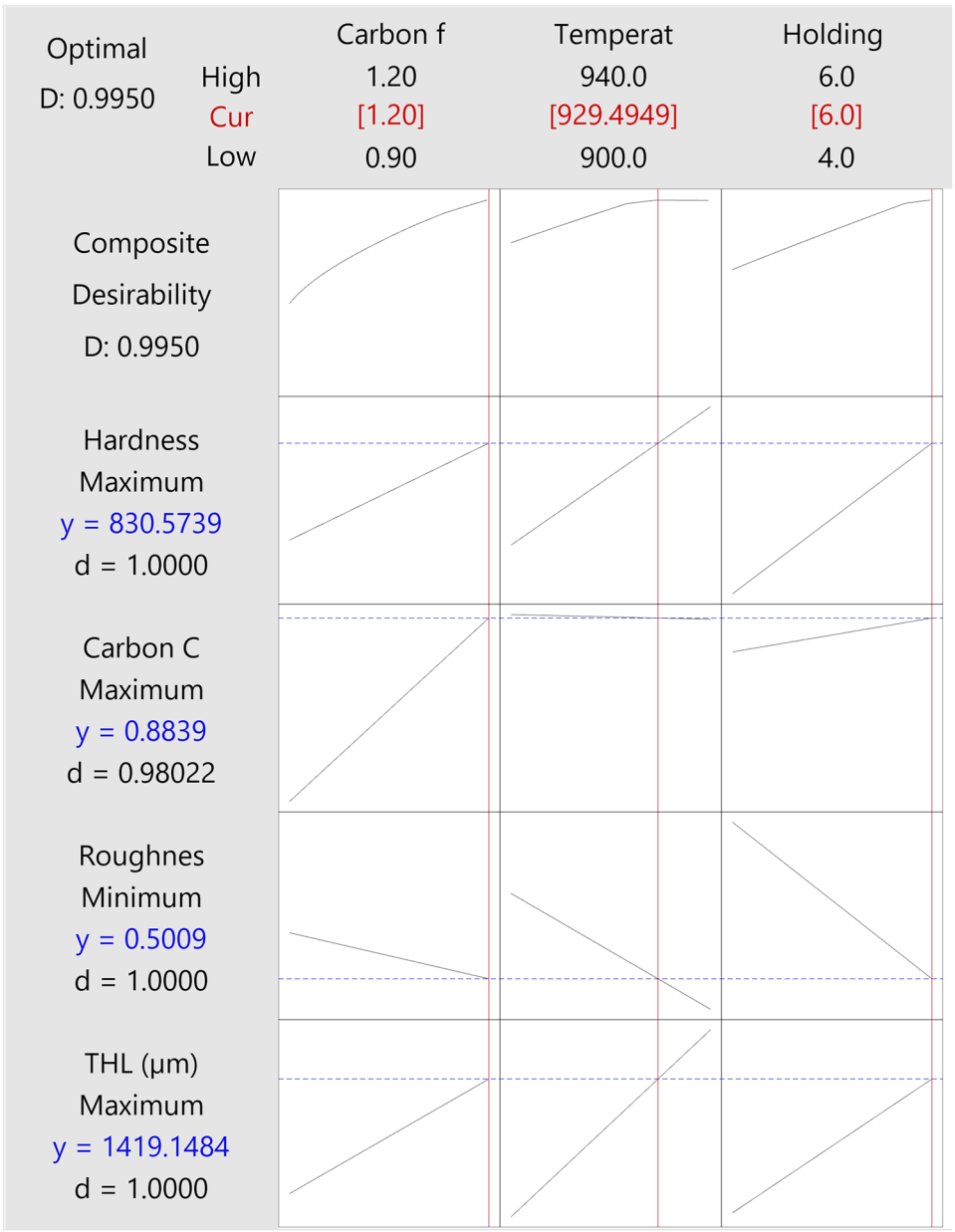

Fig. 5 Response optimization plot for carburizing gas parameters

The correlation coefficients (R^2) show that the proportion of response variation explained by the models exceed 97%, which makes them reasonably in agreement with the adjusted (R^2) and predicted (R^2) models which exceed 95% and 87% respectively.

Figure 3 shows the gas carburizing treatment tests and surface roughness on the *Y*-axis and their normalizing effects on the *X*-axis. It can be seen on the *X*-axis that the gas carburization processing parameters (carbon flow rate, temperature and holding time) exceed the normalized effect values (baseline of 2.571). Only the temperature parameter is lower than the baseline, so it is considered an insignificant parameter with 0.163 on the carbon content. Only the factors above the baseline are taken, when developing reduced regression models for all responses.

3.2 3D response surface design analysis

3D response surfaces are represented graphically to demonstrate the combination of interaction effects of the input parameters on the measured responses. Figure 4 shows the 3D responses in relation to the micro-hardness, thickness of the hardened layer, surface roughness (Ra) and carbon contents with the three combinations of significant interactions (*A*–*B*, *A*–*C* and *B*–*C*). The response surface is plotted simultaneously for two-factor, while the remaining factor takes its average value. All the interaction (*A*–*B*, *A*–*C* and *B*–*C*) shows a great effect on the responses; only the interaction of the combination (*B*–*C*) shows a minor effect on the response of carbon contents (Fig. 4d). The RSM graphs show a good agreement between the predicted and revealed values, which indicate that the developed models have a satisfactory predictive capacity.

3.3 Optimization

The linear regression method was used to choose the set of parameters for the gas carburization treatment, which leads to the maximization of micro-hardness, thickness of the hardened layer and carbon contents and at the same time to minimize the surface roughness (Ra). Three factors are used for the optimization: carbon flow rate (*A*), temperature (*B*) and holding time (*C*). According to the predicted results shown in Table 5 and confirmed in Fig. 5, the optimal value is the high value of desirability which is very close to 1 [45, 57]. The values of the desirability function make it possible to choose the best level for each parameter value to find the best case among many solutions, as shown in Table 5.

Figure 5 illustrates the best solution of optimal response values for micro-hardness, thickness of the hardened layer, carbon contents and surface roughness (Ra) that are equal to 830.57 HV, 1419.15 µm and 0.883% and 0.5 µm respectively.

Table 6 The calculation of the grey relation grade for better micro-hardness, thickness of the hardened layer, surface roughness and carbon contents

Ex no	Micro-hardness (HV)	THL (µm)	Roughness (µm)	Carbon contents (%)	Normalizing				Delta				Grey coefficient				Grey grade	Rank
					Micro-hardness (HV)	THL (µm)	Roughness (µm)	Carbon contents (%)	Micro-hardness (HV)	THL (µm)	Roughness (µm)	Carbon contents (%)	Micro-hardness (HV)	THL (µm)	Roughness (µm)	Carbon contents (%)		
1	581	1044.76	0.912	0.548	0	0	0	0	1	1	1	1	0.333	0.333	0.333	0.333	0.333	9
2	664	1175.80	0.683	0.558	0.357	0.419	0.591	0.029	0.643	0.581	0.409	0.971	0.437	0.463	0.550	0.340	0.441	7
3	782	1361.15	0.525	0.555	0.858	0.887	1	0.020	0.142	0.113	0	0.980	0.779	0.816	1	0.338	0.724	3
4	637	1110.35	0.780	0.628	0.242	0.290	0.341	0.234	0.758	0.710	0.659	0.766	0.397	0.413	0.431	0.395	0.405	8
5	751	1287.96	0.577	0.698	0.725	0.774	0.866	0.438	0.275	0.226	0.134	0.562	0.646	0.689	0.789	0.471	0.638	4
6	702	1232.61	0.705	0.613	0.518	0.613	0.535	0.190	0.482	0.387	0.465	0.810	0.509	0.564	0.518	0.382	0.479	6
7	764	1275.40	0.607	0.891	0.781	0.823	0.789	1	0.219	0.177	0.211	0	0.696	0.738	0.703	1	0.774	2
8	668	1230.37	0.730	0.812	0.373	0.435	0.470	0.771	0.627	0.565	0.530	0.229	0.444	0.470	0.486	0.686	0.515	5
9	815	1419.04	0.597	0.875	1	1	0.815	0.954	0	0	0.185	0.046	1	1	0.730	0.916	0.911	1

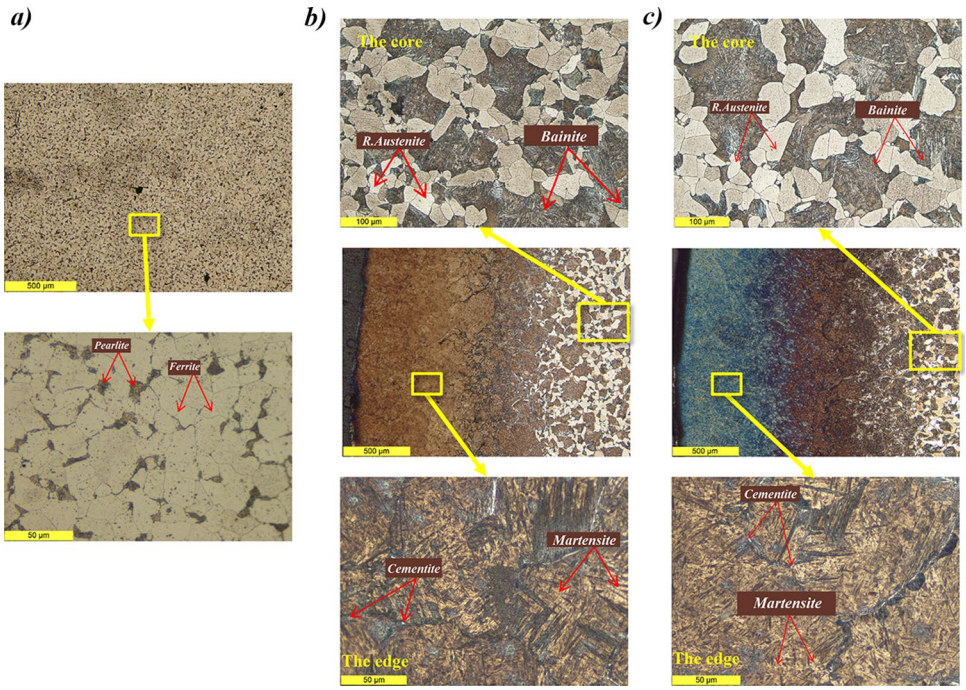

Fig. 6 Observations of the metallographic layers: **a** steel without carburizing (raw), **b** case-hardened steel (bad case), **c** case-hardened steel (best case)

They were obtained for a carbon flow rate of 1.2%, a temperature of 929.5 °C and a holding time of 6 h with composite desirability of 0.995 (very close to 1) as shown in Table 5.

The grey relational analysis (GRA) allows to optimize the four responses at the same time by a single set of process variables. Table 6 presents the results of the grey relational coefficients, grey relational scores and their ranks. The results show that the L9 test has the highest grey relational grade, which suggests that it is the most suitable condition for gas carburizing treatment for better micro-hardness, thickness of the hardened layer, surface roughness and carbon contents. In general, the higher the value of the grey relational grade, the closer the corresponding treatment parameters are to the optimal level [33, 42].

The models established in this investigation using Taguchi's method show reasonable agreement between experimental and expected values, making them competitive with many other experimental designs and approaches such as artificial neural network (ANN), genetic algorithm (GA), fuzzy, multi-objective optimization and finite element method (FEM) have been used by several researchers to model gas carburizing responses [58–61].

3.4 The microstructure of XC10 steel

After the treatment carburizing of XC10 steel, the thickness of the surface layer increases more than 35% with the increase of holding time and temperature (from about 1050 µm to more than 1400 µm), similar result was found by Boubaaya et al. [52]. Showing in the Fig. 6, the results of the enrichment of the surface layer with the carbon content demonstrate a transformation of austenite into martensite and finally a formation of cementite (Fe_3C); a same goal was obtained through many studies [16–18]. Also, there are transformations in the core of the samples, ferrite and pearlite (initial phase), that are transformed into retained austenite and bainite (after the treatment phase) [3, 20, 21]. It is also shown that when the solidification time increases, the grain size also increases. A similar microstructure was obtained by Cullen et al. [62] and Liu et al. [63]. They concluded that the different grain sizes in the material have a diverse effect. As the grain size increases, the yield strength decreases and the risk of elongation at break is much higher.

4 Conclusion

The DoE carried out in the present study according to Taguchi's L9 experimental design combined with grey relational analysis was adopted to identify the optimal parameters of the gas carburizing treatment such as holding time, carbon flow rate and temperature used to optimize the experimental responses namely the micro-hardness, thickness of the hardened layer, surface roughness (Ra) and carbon contents. The experimental results were evaluated and validated by the ANOVA analysis method. After the case carburizing treatment, we can observe the microstructure of the steel (core and edge). The main conclusions can be summarized as follows:

– The gas carburizing treatment tests show a strong optimization in micro-hardness, carbon content and surface roughness (Ra) (140%, 775% and 140%

respectively) compared to the reference values (without carburizing). Comparing the response values from the bad case to the best case, they can improve up to 40% for micro-hardness, 36% for thickness, 60% for carbon content and 53% for surface roughness (Ra).

- The models obtained showed a reasonable agreement with R^2 and R^2-predicted values which were respectively greater than 95% and 87% respectively. This shows the possibility of using these models to predict responses with satisfaction.
- The optimal responses obtained such as micro-hardness, thickness of the hardened layer, carbon contents and surface roughness (Ra) are 830.57 HV, 1419.15 µm and 0.883% and 0.5009 µm respectively, and they were obtained for a carbon flow rate with 1.2%, a temperature of 929.5 °C and a holding time of 6 h with composite desirability very close to 1.
- According to the analysis of the major effect plot of grey grade, the optimal gas carburization treatment parameters have been found for high values of carbon flow rate, a the temperature and a holding time. The results show that trial number 9 has the highest degree of grey relation, which confirms the results of the Taguchi method.
- The enrichment of the superficial layer in carbon content shows the transformation of austenite into martensite and finally into cementite (Fe_3C), which increases the thickness of the superficial by layer more than 1400 µm.
- Ultimately, the developed models in this investigation will help industries to improve the design of manufacturing processes of different products such as gears, screws, shafts, rolled plates, rollers, bands and levers.

Funding The work is financed by the Algerian Ministry of Higher education and Scientific Research (MESRS).

Declarations

Ethical approval Not applicable.

Consent to participate Not applicable.

Consent for publication Agree to publish.

Competing interests The authors declare no competing interests.

References

1. Xiao N, Hui W, Zhang Y et al (2020) High cycle fatigue behavior of a low carbon alloy steel: the influence of vacuum carburizing treatment. Eng Fail Anal 109:104215. https://doi.org/10.1016/J.ENGFAILANAL.2019.104215
2. Jo B, Sharifimehr S, Shim Y, Fatemi A (2017) Cyclic deformation and fatigue behavior of carburized automotive gear steel and predictions including multiaxial stress states. Int J Fatigue 100:454–465. https://doi.org/10.1016/J.IJFATIGUE.2016.12.023
3. Prisco U (2018) Case microstructure in induction surface hardening of steels: an overview. Int J Adv Manuf Technol 98:2619–2637. https://doi.org/10.1007/S00170-018-2412-0
4. Izciler M, Tabur M (2006) Abrasive wear behavior of different case depth gas carburized AISI 8620 gear steel. Wear 260:90–98. https://doi.org/10.1016/J.WEAR.2004.12.034
5. Meneghetti G, Terrin A, Giacometti S (2016) A twin disc test rig for contact fatigue characterization of gear materials. Procedia Struct Integr 2:3185–3193. https://doi.org/10.1016/J.PROSTR.2016.06.397
6. Burkart K, Bomas H, Zoch HW (2011) Fatigue of notched case-hardened specimens of steel SAE 5120 in the VHCF regime and application of the weakest-link concept. Int J Fatigue 33:59–68. https://doi.org/10.1016/J.IJFATIGUE.2010.07.006
7. Liu Y, Wang M, Shi J et al (2009) Fatigue properties of two case hardening steels after carburization. Int J Fatigue 31:292–299. https://doi.org/10.1016/J.IJFATIGUE.2008.08.010
8. Dong ZH, Zhang W, Kang HW et al (2020) Surface hardening of laser melting deposited 12CrNi2 alloy steel by enhanced plasma carburizing via hollow cathode discharge. Surf Coatings Technol 397:125976. https://doi.org/10.1016/J.SURFCOAT.2020.125976
9. Jiang Y, Wu Q, Wang Y et al (2019) Suppression of hydrogen absorption into 304L austenitic stainless steel by surface low temperature gas carburizing treatment. Int J Hydrogen Energy 44:24054–24064. https://doi.org/10.1016/J.IJHYDENE.2019.07.112
10. Yang Y, Yan MF, Zhang SD et al (2018) Diffusion behavior of carbon and its hardening effect on plasma carburized M50NiL steel: influences of treatment temperature and duration. Surf Coatings Technol 333:96–103. https://doi.org/10.1016/J.SURFCOAT.2017.10.068
11. Xing YZ, Wang G, Zhang Y et al (2017) Development in plasma surface diffusion techniques of Ti-6Al-4V alloy: a review. Int J Adv Manuf Technol 92:1901–1912. https://doi.org/10.1007/S00170-017-0302-5
12. Wu J, Xue W, Wang B et al (2014) Characterization of carburized layer on T8 steel fabricated by cathodic plasma electrolysis. Surf Coatings Technol 245:9–15. https://doi.org/10.1016/J.SURFCOAT.2014.02.024
13. Bataev IA, Golkovskii MG, Losinskaya AA et al (2014) Non-vacuum electron-beam carburizing and surface hardening of mild steel. Appl Surf Sci 322:6–14. https://doi.org/10.1016/J.APSUSC.2014.09.137
14. Santos D, Vasconcelos G, Abdalla AJ et al (2015) Surface characterization in a 300 M bainitic steel laser carburizing. Procedia Eng 114:322–329. https://doi.org/10.1016/J.PROENG.2015.08.075
15. Mohrbacher H (2016) Metallurgical concepts for optimized processing and properties of carburizing steel. Adv Manuf 4:105–114. https://doi.org/10.1007/s40436-016-0142-9
16. Wang KF, Sun GD, Wu YD, Zhang GH (2019) Fabrication of ultrafine and high-purity tungsten carbide powders via a carbothermic reduction–carburization process. J Alloys Compd 784:362–369. https://doi.org/10.1016/J.JALLCOM.2019.01.055
17. Benarioua Y (2018) Carburizing treatment of low alloy steels: effect of technological parameters. J Phys Conf Ser. https://doi.org/10.1088/1742-6596/1033/1/012008
18. Liu B, Wang B, Gu J (2019) Effect of ammonia addition on microstructure and wear performance of carbonitrided high carbon bearing steel AISI 52100. Surf Coatings Technol 361:112–118. https://doi.org/10.1016/j.surfcoat.2019.01.019

19. Li GM, Liang YL, Yin CH et al (2019) Study of M50NiL steel under carburizing and nitriding duplex treatment. Surf Coatings Technol 375:132–142. https://doi.org/10.1016/j.surfcoat.2019.07.017
20. Pashangeh S, Zarchi HRK, Banadkouki SSG, Somani MC (2019) Detection and estimation of retained austenite in a high strength Si-bearing bainite-martensite-retained austenite micro-composite steel after quenching and bainitic holding (Q&B). Metals (Basel) 9:1–21. https://doi.org/10.3390/met9050492
21. Hiremath P, Sharma S, Gowrishankar MC et al (2020) Effect of post carburizing treatments on residual stress distribution in plain carbon and alloy steels - a numerical analysis. J Mater Res Technol 9:8439–8450. https://doi.org/10.1016/j.jmrt.2020.05.104
22. Abdenour S, Linda A, Oualid C et al (2021) Influence of the carburization time on the structural and mechanical properties of XC20 steel. Mater Res Express 8:1–13. https://doi.org/10.1088/2053-1591/ac1ece
23. Zhao Y, Tan Y, Ji X et al (2018) In situ study of cementite deformation and its fracture mechanism in pearlitic steels. Mater Sci Eng A 731:93–101. https://doi.org/10.1016/J.MSEA.2018.05.114
24. Song Y, Han Z, Chai M et al (2018) Effect of cementite on the hydrogen diffusion/trap characteristics of 2.25Cr-1Mo-0.25V steel with and without annealing. Materials (Basel) 11:1–15. https://doi.org/10.3390/ma11050788
25. Li C, He Q, Tang W, Lu F (2004) Carburising of steel AISI 1010 by using a cathode arc plasma process. Surf Coatings Technol 187:1–5. https://doi.org/10.1016/J.SURFCOAT.2004.01.026
26. Yan MF, Liu ZR (2001) Study on microstructure and microhardness in surface layer of 20CrMnTi steel carburised at 880 °C with and without RE. Mater Chem Phys 72:97–100. https://doi.org/10.1016/S0254-0584(01)00321-2
27. Kargar F, Laleh M, Shahrabi T, Rouhaghdam AS (2014) Effect of treatment time on characterization and properties of nanocrystalline surface layer in copper induced by surface 37:1087–1094
28. Gressmann T, Nikolussi M, Leineweber A, Mittemeijer EJ (2006) Formation of massive cementite layers on iron by ferritic carburising in the additional presence of ammonia. Scr Mater 55:723–726. https://doi.org/10.1016/J.SCRIPTAMAT.2006.06.022
29. Britton WM, Clarke A, Evans HP (2021) A novel method for automatic detection of incipient micropitting in ground surfaces. Tribol Int 159:106959. https://doi.org/10.1016/J.TRIBOINT.2021.106959
30. Vrcek A, Hultqvist T, Baubet Y et al (2019) Micro-pitting and wear assessment of engine oils operating under boundary lubrication conditions. Tribol Int 129:338–346. https://doi.org/10.1016/J.TRIBOINT.2018.08.032
31. Liu Z, Peng Y, Chen C et al (2020) Effect of surface nanocrystallization on low-temperature gas carburization for AISI 316L austenitic stainless steel. Int J Press Vessel Pip 182:104053. https://doi.org/10.1016/J.IJPVP.2020.104053
32. Roy S, White D, Sundararajan S (2018) Correlation between evolution of surface roughness parameters and micropitting of carburized steel under boundary lubrication condition. Surf Coatings Technol 350:445–452. https://doi.org/10.1016/J.SURFCOAT.2018.05.083
33. Nguyen PH, Banh TL, Mashood KA et al (2020) Application of TGRA-based optimisation for machinability of high-chromium tool steel in the EDM process. Arab J Sci Eng 45:5555–5562. https://doi.org/10.1007/s13369-020-04456-z
34. Asif M, Tariq A (2019) Estimation of thermal contact conductance using transient approach with inverse heat conduction problem. Heat Mass Transf 55:3243–3264. https://doi.org/10.1007/s00231-019-02617-x
35. Badkar DS, Pandey KS, Buvanashekaran G (2010) Parameter optimization of laser transformation hardening by using Taguchi method and utility concept. Int J Adv Manuf Technol 52:1067–1077. https://doi.org/10.1007/S00170-010-2787-Z
36. Senthilkumar N, Tamizharasan T, Anandakrishnan V (2014) Experimental investigation and performance analysis of cemented carbide inserts of different geometries using Taguchi based grey relational analysis. Meas J Int Meas Confed 58:520–536. https://doi.org/10.1016/j.measurement.2014.09.025
37. Agboola OO, Ikubanni PP, Adeleke AA et al (2020) Optimization of heat treatment parameters of medium carbon steel quenched in different media using Taguchi method and grey relational analysis. Heliyon 6:e04444. https://doi.org/10.1016/j.heliyon.2020.e04444
38. Touati S, Mekhilef S (2017) Statistical analysis of surface roughness in turning based on cutting parameters and tool vibrations with response surface methodology (RSM). Mater Tech 105:401. https://doi.org/10.1051/mattech/2017037
39. Hu Y, Yang J, Wang J, Wang Q (2018) Investigation of hydrodynamic and heat transfer performances in grille-sphere composite pebble beds with DEM-CFD-Taguchi method. Energy 155:909–920. https://doi.org/10.1016/j.energy.2018.05.018
40. Naqiuddin NH, Saw LH, Yew MC et al (2018) Numerical investigation for optimizing segmented micro-channel heat sink by Taguchi-Grey method. Appl Energy 222:437–450. https://doi.org/10.1016/j.apenergy.2018.03.186
41. Kabnure BB, Shinde VD, Kolhapure RR (2018) Optimization to develop multiple response microstructure and hardness of ductile iron casting by using GRA. J Inst Eng Ser D 99:235–243. https://doi.org/10.1007/s40033-018-0161-8
42. Panda A, Sahoo AK, Rout AK (2016) Multi-attribute decision making parametric optimization and modeling in hard turning using ceramic insert through grey relational analysis: a case study. Decis Sci Lett 5:581–592. https://doi.org/10.5267/j.dsl.2016.3.001
43. Sproge L (1988) Ågren J (1988) Experimental and theoretical studies of gas consumption in the gas carburizing process. J Heat Treat 61(6):9–19. https://doi.org/10.1007/BF02833160
44. Bhadeshia HKDH (2010) (2010) A commentary on: Diffusion of carbon in austenite with a discontinuity in composition. Metall Mater Trans A 417(41):1605–1615. https://doi.org/10.1007/S11661-010-0276-5
45. Bezazi A, Boumediri H, Garcia G, Bezzazi B (2020) Alkali treatment effect on physicochemical and tensile properties of date palm rachis fibers. J Nat Fibers 19:1
46. Del Pino GG, Bezazi A, Boumediri H et al (2021) Optimal tensile properties of biocomposites made of treated Amazonian curauá fibres using Taguchi method. Mater Res 24:20210326. https://doi.org/10.1590/1980-5373-MR-2021-0326
47. Abdulkadir LN, Abou-el-hossein K, Abioye AM, Liman MM (2019) Process parameter selection for optical silicon considering both experimental and AE results using Taguchi L9 orthogonal design. Int J Adv Manuf Technol 103:4355–4367
48. Laouissi A, Nouioua M, Yallese MA et al (2021) Machinability study and ANN-MOALO-based multi-response optimization during eco-friendly machining of EN-GJL-250 cast iron. Int J Adv Manuf Technol 117:1179–1192. https://doi.org/10.1007/S00170-021-07759-Z/FIGURES/7
49. Kasman Ş (2013) Multi-response optimization using the Taguchi-based grey relational analysis: a case study for dissimilar friction stir butt welding of AA6082-T6/AA5754-H111. Int J Adv Manuf Technol 68:795–804. https://doi.org/10.1007/S00170-012-4720-0
50. Duan HQ, Han YF, LÜ WJ et al (2016) Effect of solid carburization on surface microstructure and hardness of Ti-6Al-4V alloy and (TiB+La2O3)/Ti-6Al-4V composite. Trans Nonferrous Met Soc China 26:1871–1877. https://doi.org/10.1016/S1003-6326(16)64301-7
51. Aramidea FO, Ibitoye SA, Oladele IO, Borode JO (2009) Effects of carburization time and temperature on the mechanical properties of carburized mild steel, using activated carbon as carburizer. Mater Res 12:483–487. https://doi.org/10.1590/S1516-14392009000400018

52. Boubaaya R, Allaoui O, Benarioua Y, Driss Z (2020) Effect of the carburizing layer on the morphology of chromium carbides. J Sib Fed Univ Eng Technol 13:187–193. https://doi.org/10.17516/1999-494x-0215
53. Hiremath P, Sharma S, Gowrishankar MC et al (2020) Effect of post carburizing treatments on residual stress distribution in plain carbon and alloy steels – a numerical analysis. J Mater Res Technol 9:8439–8450. https://doi.org/10.1016/J.JMRT.2020.05.104
54. Oyetunji A, Adeosun SO (2012) Effects of carburizing process variables on mechanical and chemical properties of carburized mild steel. J Basic Appl Sci 8:319–324. https://doi.org/10.6000/1927-5129.2012.08.02.11
55. Dechow PM, Douglas JS (2000) Reproduced with permission of the copyright owner. Further reproduction prohibited without. J Allergy Clin Immunol 130:556
56. Oyetunji A (2012) Effects of carburizing process variables on mechanical and chemical properties of carburized mild steel. J Basic Appl Sci 8:319–324. https://doi.org/10.6000/1927-5129.2012.08.02.11
57. Bouhemame N, Aiadi KE, Bezazi A et al (2021) Tensile properties optimization of date palm leaflets using Taguchi method. J Nat Fibers 19:1. https://doi.org/10.1080/15440478.2021.1916674
58. Liang R, Wang Z, Yang S, Chen W (2021) Study on hardness prediction and parameter optimization for carburizing and quenching: an approach based on FEM. ANN and GA Mater Res Express 8:116501. https://doi.org/10.1088/2053-1591/AC3279
59. Mahto R, Kumar S, Kumar S, Kumar P (2017) Optimization of heat treatment process parameter using Taguchi and fussy logic approach in bearing manufacturing industry. Int Res J Eng Technol 04
60. Cavaliere P, Perrone A, Silvello A (2015) FEM and multi-objective optimization of steel case hardening. J Manuf Process 17:9–27. https://doi.org/10.1016/J.JMAPRO.2014.10.005
61. Hanza SS, Marohnić T, Iljkić D, Basan R (2021) Artificial neural networks-based prediction of hardness of low-alloy steels using specific Jominy distance. Met 11:714. https://doi.org/10.3390/MET11050714
62. Cullen MM, Kazeem OS, Olukayode LA, Graeme JO (2014) Microstructural features and mechanical behaviour of unalloyed medium carbon steel (EN8 steel) after subsequent heat treatment. Proc World Congr Eng Comput Sci
63. Liu H, Dong Y, Zheng H et al (2021) Precipitation criterion for inhibiting austenite grain coarsening during carburization of Al-containing 20Cr gear steels. Met 11:504. https://doi.org/10.3390/MET11030504